

## CHAPTER 5

# Test Facilities and Other Project R&D Programs

### 5.1 TESLA

In this section a brief description of the test facilities for the TESLA linear collider, the main achievements to date, and the future R&D program are given. Additional information on the superconducting linac technology can be found in the TESLA machine overview chapter (Chapter 3).

The development program for the TESLA technology is centered at the test facility at DESY (TTF) and has been pursued from the beginning by a broad international collaboration (initiated by the late Bjørn H. Wiik in 1992). To date, the TESLA collaboration has 44 members from 11 countries (Armenia, China, Finland, France, Germany, Italy, Poland, Russia, Switzerland, United Kingdom and USA). The TTF (Figure 5.1) includes infrastructure labs and shops for superconducting cavity treatment, test stands and the accelerator module assembly as well as a test linac for an integrated system test of the TESLA accelerator prototype with beam. Two more test facilities, focused mainly on the generation of high quality electron beams with photocathode rf guns, exist at FNAL (A0 facility) and DESY-Zeuthen (PITZ facility). At A0 the generation of flat (large ratio of horizontal to vertical emittance) electron beams using an innovative beam optics scheme were experimentally demonstrated for the first time in May 2000.

The processing of the cavities fabricated in industry involves chemical etching of the inner surfaces, high temperature treatment at 1400°C, and high pressure rinsing with ultra-pure water. Recently, electropolishing (EP) was shown to be a very successful method to achieve cavities with excellent performance. This method, pioneered at KEK, is developed in collaboration with CERN and KEK. High quality clean rooms provide a dust-free environment during the treatment and assembly procedures. All cavities undergo a quality test (measurement of  $Q_0$  versus gradient) in a vertical bath cryostat at 2 K with continuous wave (CW) rf excitation. Some of the cavities are also tested with pulsed rf after assembly of the main power and higher order mode (HOM) couplers. So far, nearly one hundred 9-cell cavities and a number of shorter structures have been processed and tested at TTF. The evolution of cavity performance on the test stand over a period of six years is shown in

## TESLA TEST FACILITY (HALL 3)

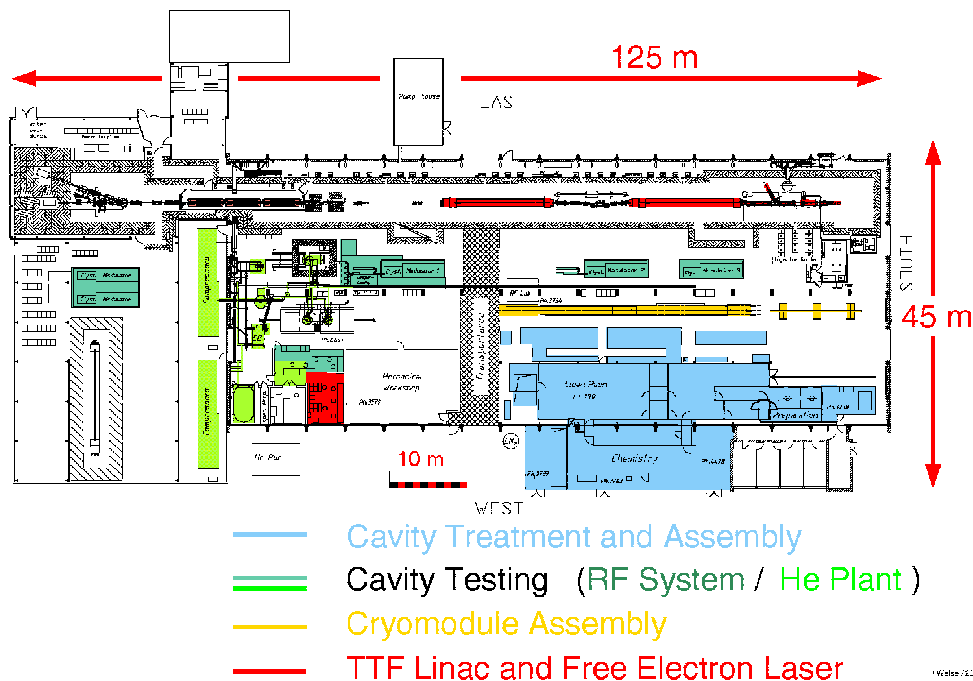


FIGURE 5.1. Layout of the TESLA Test Facility at DESY.

Figure 5.2. The two data sets shown differentiate between the performance obtained when cavities were tested for the first time and the performance after additional processing (best test). In view of future large scale production, it is particularly important that the TESLA 500 GeV design gradient has on average already been surpassed in the first test, *i.e.*, with cavities having gone through the standard treatment only once without having to be returned to the shops for additional processing. This proves that the superconducting cavity technology is mature for mass production of these accelerator structures at the required gradient of 23.8 MV/m with sufficient reliability and reproducibility. The present cavity R&D program is focused on pushing the routinely achievable gradients to higher values in order to secure the energy upgradability of the TESLA linac. The results obtained with the EP treatment for short structures (several single cell resonators reached gradients above 40 MV/m) let this method appear to be the most promising candidate for further improvement of the Niobium surface and thus the maximum accelerating field. In context with the ongoing EP R&D program, but not fundamentally linked to it, it was also found that a bakeout at very moderate temperature (typically 120°C) can be very effective to avoid a drop in the quality factor at high gradients. Application of these methods to 9-cell cavities has just started and already produced the best 9-cell cavity ever tested at TTF (see Figure 5.3). As this report is being written, another six cavities have reached gradients between 31 and 35 MV/m. More experience will be gained in the near future, and eventually an entire accelerator module with electropolished cavities will be constructed and

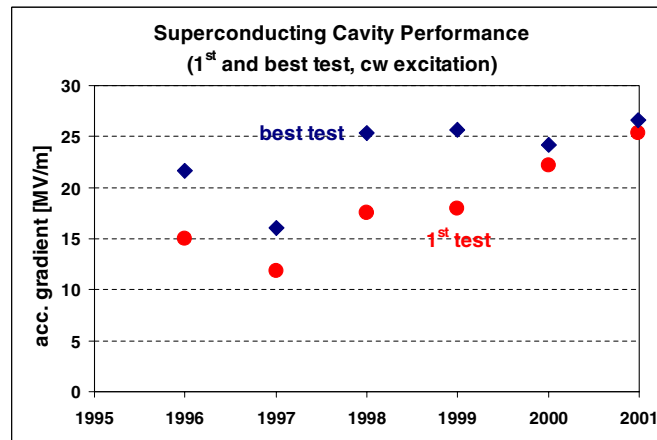


FIGURE 5.2. Evolution of the average gradient obtained with 9-cell cavities in CW-tests in the years 1995 to 2000 (the time on the horizontal axis refers to the preceding 12 month period, over which the test results have been averaged). Both data for first test and best test (after additional treatment) are shown.

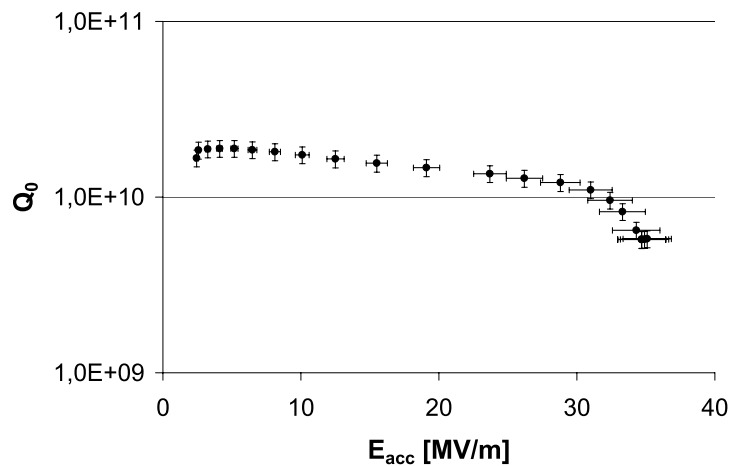


FIGURE 5.3. Performance (quality factor versus gradient) of a 9-cell electro-polished cavity on the CW test stand, March 2002.

tested. This module will also include the piezo-tuner device to compensate for Lorentz-force detuning, which has already been successfully demonstrated in a 9-cell cavity at 23.5 MV/m.

The linear accelerator at TTF serves two purposes: first, it provides an integrated system test of the TESLA linac components with beam and second, it is used as a driver for a SASE FEL in the VUV wavelength regime. This two-fold use of the TTF linac occasionally makes scheduling of beam time more complicated than for a single-purpose facility. However, there are benefits and synergies which outweigh these complications, such as having the same

## TEST FACILITIES AND OTHER PROJECT R&D PROGRAMS

operations crew for both FEL and linac technology oriented studies, and the need for a highly reliable around-the-clock operation for the FEL users as an efficient motivation and driving force to achieve this reliability in all technical components of the linac.

Operation of the linac began in May 1997 with the first accelerator module. So far, three modules have been tested with beam (at present, modules 2 and 3 are installed and in operation). The photocathode rf gun injector is capable of delivering bunch trains with parameters very close to the TESLA linear collider specifications in terms of beam current and pulse length. It also delivers bunches with sufficiently low emittance for successful operation of the FEL. A full description of the experience gained at the TTF linac in its first phase of operation (TTF-I for short) is beyond the scope of this brief overview. Among the highlights of most recent operation are the achievement of saturation at the FEL, a first successful phase of routine operation for users of the FEL photon beam, and continuous operation with accelerating gradient (21 MV/m), beam current (7–8 mA) and pulse length (0.8 ms) near the TESLA design values. While the linac rf is operated at 5 Hz repetition rate, the beam repetition rate has up-to-date been limited to 1 Hz because of insufficient stability of the photocathode rf gun.

The TTF-I program is being concluded in autumn 2002. The last tests are devoted to one more accelerator module (named module 1\*, because it is the original module 1 equipped with new cavities), which is expected to yield an average accelerating gradient of 25 MV/m, and to a beam test with a first version of the so-called superstructure concept. In a superstructure, two cavities are fed with rf power by a single coupler which saves length (the fill factor is increased by 6% in comparison with the present TTF modules) and cost by reducing the number of couplers. First beam tests with two superstructures at a gradient of 15 MV/m have been performed successfully, proving the principle of this concept and confirming very satisfactory damping of higher order modes in the structures. After completion of that experimental program, the linac will be lengthened by three more modules (two of which contain only cavities which have reached 25 MV/m or more on the test stand) in an already completed additional tunnel, and the FEL installations will be modified to prepare for the second phase (TTF-II) of the user facility, commissioning of which will begin in the second half of 2003. An overview of the TTF milestone plan, together with a summary of the milestones reached during the TESLA R&D program, is given in Table 5.1.

TABLE 5.1

Milestones reached during the TESLA R&amp;D program and schedule for the near future.

Date	Milestone
1992	TESLA Collaboration established
1994	5-cell cavities reach 25 MV/m at Cornell
1995	First TESLA 9-cell cavity reaches 25 MV/m
May 1997	Beam accelerated in first TTF module at 16 MV/m
January 1999	FNAL rf gun in operation at TTF
February 1999	Second TTF module at 20 MV/m
September 1999	Third TTF module at 22 MV/m
1999/2000	Average gradient of TESLA cavities exceeds 25 MV/m on test stand
February 2000	First lasing of TTF FEL at 108 nm wavelength
May 2000	Demonstration of flat-beam electron source at FNAL-A0
March 2001	Publication of the TESLA TDR
September 2001	TTF FEL demonstrates power gain of $10^7$ in saturation at 80–120 nm wavelength
Autumn 2001	Beginning of experimental user program with FEL photon beam
January 2002	First beam at PITZ rf gun
March 2002	Electro-polished 9-cell cavity reaches 35 MV/m
Spring 2002	Routine operation of TTF linac with high up-time ( $\sim 90\%$ ) near TESLA design parameters
July–Sept. 2002	Test of superstructure
July–Oct. 2002	High gradient test of 4 <sup>th</sup> module (module 1*)
November 2002	Beginning of extension of TTF linac to five modules (40 cavities) in total
Spring 2003	RF test of new modules 4 and 5
Second half 2003	Commissioning of TTF Phase-II

## 5.2 JLC-C

The ATF at KEK will also serve as a facility for an injector study of JLC-C because the beam parameters of JLC-C are almost identical to those of JLC-X/NLC. On the other hand, no special test facility for the main linac rf system for JLC-C is being planned. However, an FEL SASE source called SCSS (SPRING-8 Compact SASE Source) is under construction at SPRING-8 in Japan since 2001. Its rf system is almost identical to that of JLC-C so that it indeed serves as a test facility for the JLC-C. The high power test of the components including the accelerator structure and the pulse compressor will be done by

## TEST FACILITIES AND OTHER PROJECT R&D PROGRAMS

March 2003. The beam acceleration up to 500 MeV will start in the second half of 2005. 1 GeV will be reached in the second half of 2006. (These dates are subject to change due to the re-organization of SPring-8.) The layout is schematically depicted in Figure 5.4.

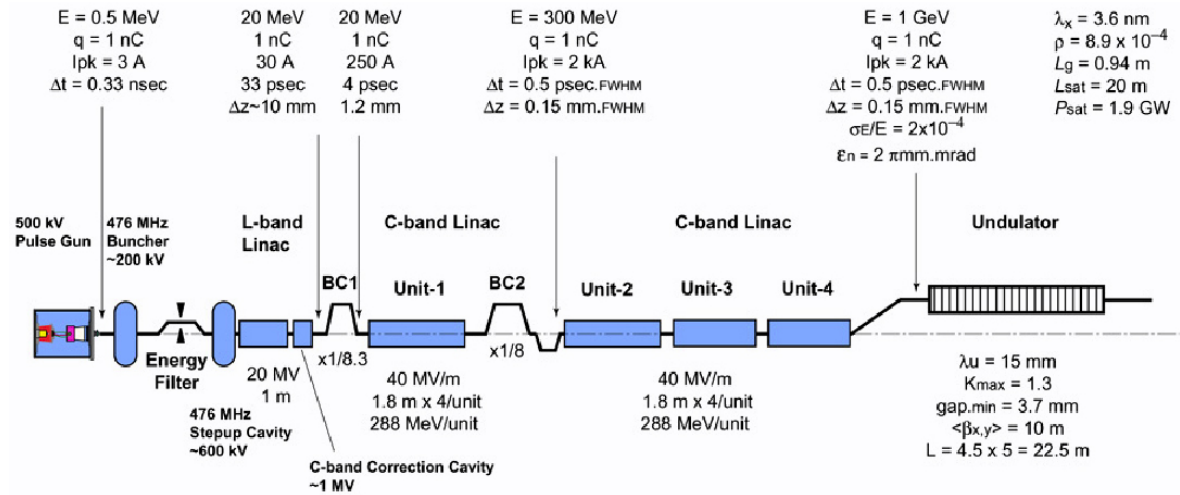


FIGURE 5.4. Layout of the first stage of SCSS.

The acceleration scenario beyond the injector is as follows:

- The electron beam parameters at the end of the first bunch compressor (BC1) are: Energy 20 MeV, bunch charge 1 nC, bunch-to-bunch spacing 2.1 ns, train length 300 ns, bunch length 4 ps (FWHM).
- The first C-band rf unit (8 m) accelerates the beam to 300 MeV.
- The second bunch compressor (BC2) compresses the bunch length to 0.5 ps (FWHM,  $\sigma_z \sim 80 \mu\text{m}$ ).
- Three C-band units (Units 2, 3, and 4) accelerate the beam to 1 GeV. The unloaded gradient in all the C-band cavities is 40 MV/m.

The first stage of SCSS will verify the performance of the following items for the JLC-C:

- RF system test as a whole, including the beam up to the full accelerating gradient.
- High power properties of the pulse compressor and the choke-mode cavity.
- RF BPM resolution and accuracy.
- Multibunch operation (this is not essential for SASE, but the same beam train length as for JLC-C has been chosen.)

There are still some differences from the JLC-C rf system:

- Solenoid-focusing klystrons are used in the SCSS.
- Multibunch beam dynamics studies are insufficient because the emittance of SCSS is 100 times larger than the vertical emittance of JLC-C and the number of rf units is much smaller. Also there is a minor difference in the bunch-to-bunch spacing (1.4 ns in JLC-C and 2.1 ns in SCSS).

### 5.3 JLC-X/NLC

The primary rf R&D program is centered around the NLC Test Accelerator with the accelerator structure development and the SLED-II demonstration. However, the JLC-X/NLC incorporates a very broad R&D program on luminosity related issues as well. These include the ATF prototype damping ring at KEK, the ASSET and Collimator Wakefield Test facilities at SLAC, and the Stabilization Demonstrations. In addition, the largest linear collider test facility that has been constructed was the Stanford Linear Collider (SLC). This facility was built with the dual purpose of demonstrating the feasibility of a linear collider while studying the  $Z^0$  boson.

The SLC contained all of the same subsystems that exist in the next-generation linear colliders: a positron source, a polarized electron source, damping rings, bunch compressors, a main linac, a beam collimation system, and final foci with beam extraction lines. In addition, as will be needed in a future collider, the SLC contained extensive emittance diagnostics and many beam feedback loops that automated much of the required beam tuning. A schematic is shown in Figure 5.5.

The SLC was proposed in 1980 and construction started in 1983 with commissioning beginning in 1987. After two difficult years of commissioning, the first  $Z^0$  was seen at the IP in 1989. A steady stream of improvements were made to the collider over the following decade including: over 50 beam size (wire) monitors to diagnose the sources of emittance dilution, beam collimators and muon spoilers to reduce backgrounds in the detector, new damping ring vacuum chambers to improve the extracted beam stability, and constant replacements of hardware that was not sufficiently reliable or stable. In addition, many new techniques were developed including: BNS damping to control the Beam BreakUp instability, new beam steering methods such as Two-Beam Dispersion Free Steering, and beam-beam deflection scans and dither feedbacks to tune the beam delivery system. In the end, the collider was operating near its design luminosity but in a parameter regime very different from that initially conceived; a plot of the beam sizes at the IP is shown in Figure 5.6. The success of the SLC is a true credit to the creativity and dedication of the large number of people who worked on it, as well as the inventiveness and audacity of its progenitors. It is also worth noting that, although the difficulties encountered when commissioning the SLC were much larger than anticipated, the single best measurement of  $\sin^2\theta_W$  was still made at this facility.

Many of the detailed experiences from the SLC are either not applicable or have already been incorporated into the next-generation designs. However, it should be noted that the tolerances in the SLC were *looser* than in *any* of the current linear collider proposals

TEST FACILITIES AND OTHER PROJECT R&D PROGRAMS

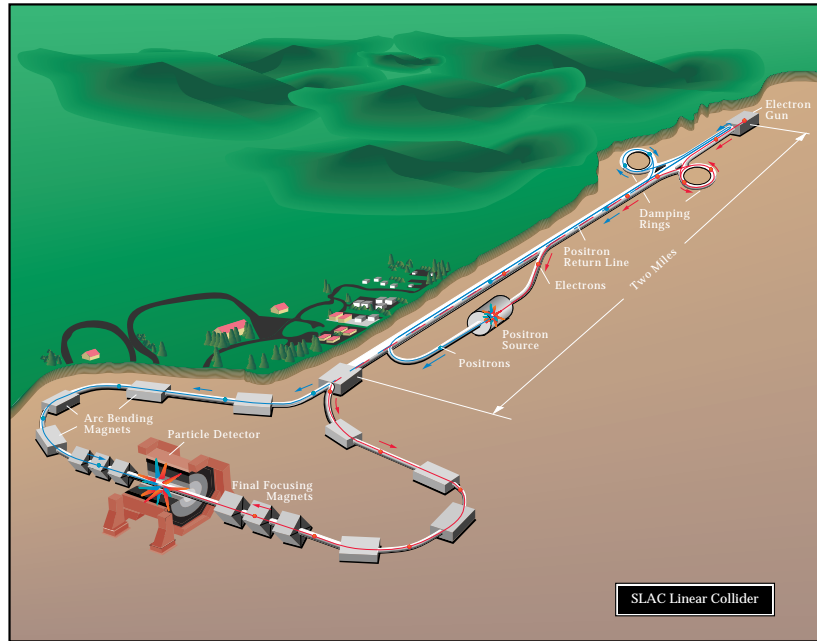


FIGURE 5.5. Schematic of the Stanford Linear Collider.

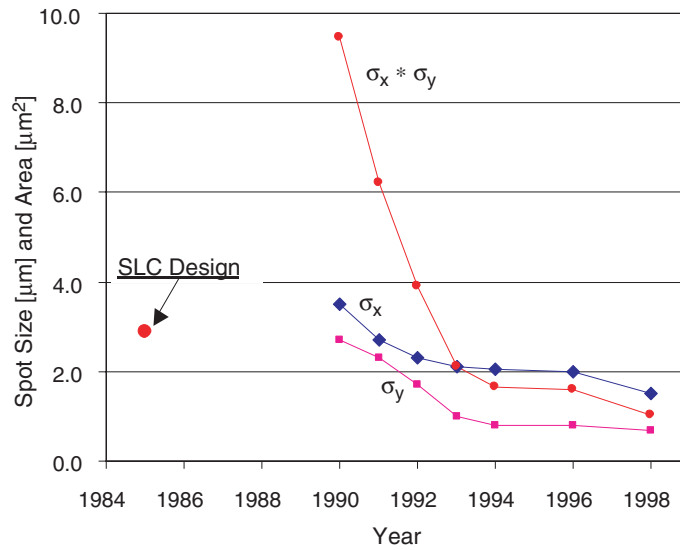


FIGURE 5.6. Spot sizes and cross-sectional area at the SLC IP as a function of time from 1990 through 1998; the design spot sizes were 1.7 μm by 1.7 μm.

and the difficulties of these future colliders should not be minimized. In particular, there are still a number of more global “lessons” that are important to remember. First, a linear collider lacks the inherent stability of the storage ring—every rf pulse differs from the previous, making hardware and beam stability, especially from the sources and the damping rings, essential. Next, reliable hardware is mandatory as demonstrated by the experience with the SLC, and more recently with the Tevatron and HERA. If the hardware interruptions are too frequent, then the collider is not up long enough to make effective progress on the luminosity. It was only after the SLC achieved reasonable reliability that the many beam tuning challenges for a linear collider could be addressed. Third, noninvasive diagnostics are needed often to determine hardware problems as well as beam physics issues. Of course, BPM’s are placed throughout in all designs but the 50+ beam size monitors in the SLC allowed rapid localization and diagnosis of subtle hardware problems that would have been hard to trace otherwise. Finally, simulations do not accurately represent the true difficulty of operating the beams and tuning the luminosity. It is important to allow for multiple backup tuning solutions as well as parameter flexibility because the biggest difficulties that will likely be encountered are those that are not yet considered or simulated.

Beyond the SLC, many additional test facilities have been created at KEK and SLAC to specifically validate the X-band linear collider design. These include: the NLC Test Accelerator (NLCTA), which is an rf systems test; the Final Focus Test Beam (FFTB), which studied the issue of focusing the beam to the very small spot sizes needed to attain the desired luminosity; the Accelerator Test Facility, which is a prototype damping ring for a normal-conducting linear collider; the Accelerator Structure SETup (ASSET), which is used to directly measure the long-range transverse wakefields; the Collimator Wakefield Test, which is used to measure the short-range wakefields from beam collimator-like devices; and the Stabilization Demonstrations, which have quantified the expected stability, have stabilized a 100 kg block, and will demonstrate the required stabilization in an IR-like environment.

It should be noted that most of these facilities are dedicated to studying issues related to luminosity—only the NLCTA is devoted to the rf system goals. Although the rf system is the most visible of the technological components required for a linear collider, it is also relatively straightforward to validate. A small systems test of 0.1–1% of the rf system is all that is really needed. In contrast, validating the damping ring concepts, the particle sources, the emittance preservation, or the beam delivery system could be a much more daunting task. Fortunately, the normal-conducting designs allow the linear collider subsystems to be based on other operating accelerators or accelerator subsystems as well as making use of the essential experience from the SLC. In particular, the polarized electron source and the positron production system are modest extensions of the SLC sources. The damping rings are similar to third-generation synchrotron light sources and are required to produce an equilibrium emittance that is only a factor of 2 below what has been achieved at the Advanced Light Source (ALS) in Berkeley or the ATF at KEK. The bunch compressor is based on experience from the SLC bunch compressor and is similar to, although not as difficult, as the bunch compressors for the new SASE-based short wavelength FEL drivers. Much of the emittance preservation techniques and the final focus systems were demonstrated at the SLC and the Final Focus Test Beam (FFTB).

### 5.3.1 NLC Test Accelerator

The Next Linear Collider Test Accelerator (NLCTA) has been a testing ground for the X-band rf system components and has demonstrated the viability of an early version of the NLC rf system. The facility was proposed in the early 1990s to provide system integration testing of the NLC X-band rf components being developed at SLAC and KEK while these systems were still in an early stage of development. The design philosophy was to make it large enough to yield meaningful operating statistics, and to make it capable of accelerating an NLC-like beam to verify performance, especially in regard to the beam loading compensation. The system was rapidly commissioned and in 1997 accelerated beam to 350 MeV while demonstrating the desired beam loading compensation. The system was upgraded in 1999 to deliver twice the rf power to structures to be able to generate higher acceleration gradients, and the rf control system was upgraded to allow around-the-clock unmanned operation.

The rf system design of the NLCTA is similar to that proposed in the 1996 NLC ZDR. The initial implementation of the NLCTA contained four rf stations (including the injector), each of which consisted of a modulator powering a single 50 MW klystron which drove a SLED-II pulse compression system. The SLED-II pulse compression systems compressed the  $1.5 \mu\text{s}$  klystron pulses by a factor of 6 in time and gained a factor of 4 in peak power. The resulting 200 MW, 240 ns pulses in the NLCTA powered two 1.8 m long X-band accelerator structures (100 ns fill time) to produce  $\sim 50 \text{ MV/m}$  unloaded gradients.

A schematic of the NLC Test Accelerator is shown in Figure 5.7. The fourth rf station shown in the figure was later eliminated from the plan. The first rf station is used to power the injector, which was designed to generate beams with NLC-like currents ( $\sim 1 \text{ A}$ ), but with the bunch spacing equal to the X-band period (88 ps). The beam source is a 150 kV, thermionic DC gun, and the injector is followed by a chicane that allows for collimation of the longitudinal bunch tails generated by the direct DC-to-X-Band bunching. The two accelerator structures used in the injector are half the nominal length to reduce the beam loading and allow for higher currents which compensate the collimation losses in the chicane (typically  $1/3$ ). To improve the bunching efficiency, the first structure has a low beta section in its upstream end and is preceded by two pre-bunching cavities, all powered from the SLED-II pulse.

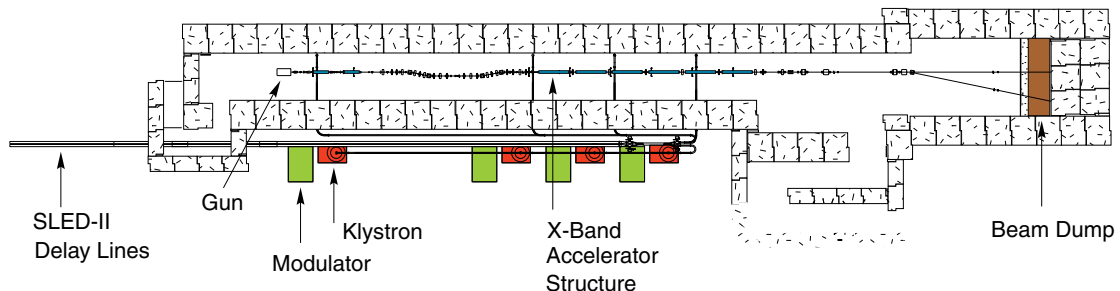


FIGURE 5.7. Schematic of the NLC Test Accelerator.

The injector was commissioned in late 1996 and, by the end of 1997, both linac rf stations were operational and the pairs of 1.8 m structures were typically run at unloaded gradients of 44 MV/m in the first station and 37 MV/m in the second station. At these levels, beam-loading compensation measurements were made that demonstrated 17% compensation to within the 0.3% level required for the NLC. The facility delivered beam with a peak energy of roughly 350 MeV. A photograph of the beam line, with the four 1.8-m accelerator structures after the injector, is shown in Figure 5.8.



FIGURE 5.8. Photograph of the beam line in the NLC Test Accelerator.

Subsequent operation brought the gradients up to the 50 MV/m design value but the maximum gradients were limited by rf breakdown. The standard processing technique is to process to higher than nominal gradient and then reduce the gradient for operation. However, to achieve higher gradients, upgrades to the rf stations were required. During a two to three year period, both of the linac modulators were partially rebuilt, some of the SLED-II components replaced with ones capable of handling higher peak power, and a second 50 MW XL4 klystron was added to each station. Also, an automated rf processing system was developed and the machine protection system improved to allow for around-the-clock, unmanned structure processing.

During this period, the NLCTA program focused on processing one of the Damped-Detuned Structures (DDS) to 73 MV/m with 240 ns pulses. After roughly 1000 hours of processing at 60 Hz, it became clear that stable operation at such a gradient would not be attainable. Also, *in situ* beam-based measurements of the structure phase advance profile revealed large changes, suggesting substantial erosion of copper, in the upstream structure irises. The 1.8-m accelerator structures are nearly constant-gradient structures and thus the iris radii and the rate of rf power flow is large at the upstream end. Subsequent measurements

## TEST FACILITIES AND OTHER PROJECT R&D PROGRAMS

of the other structures in the NLCTA showed similar patterns of damage occurring at gradients as low as 50 MV/m. This prompted an aggressive program to develop more robust high-gradient structures.

Before operating the relatively long 1.8-m prototype structures, many shorter X-band accelerator structures had been processed to much higher gradients. Single cell standing-wave cavities had operated at 150–200 MV/m and a short 20 cm structure had operated at 120–150 MV/m. In addition to being much shorter than the prototype 1.8-m structures, all of these structures had much lower rates of rf power flowing through the structure. Given this previous experience and the observed pattern of damage in the 1.8-m structures, where only the upstream end seemed to be affected, it was hypothesized that the damage was related to the group velocity of the rf power flowing through the structure. To study this idea, the first test structure was constructed by cutting off the last 1/3 of the DS2 structure, so that the maximum group velocity was 5% instead of 12% of  $c$ , and brazing on a new input coupler. This structure rapidly processed  $\sim 65$  MV/m.

Next, a series of test accelerator structures were constructed to explore the dependence of the damage and breakdown on both the structure length and on the group velocity of the rf power through the structure. Both traveling-wave and short standing-wave structures were built and tested. In addition, new processing, cleaning, and handling procedures were implemented. While these tests confirmed the initial hypothesis that there is a strong correlation between the group velocity and the breakdown/damage gradient levels, the test structures were still limited to operating at gradients of  $\sim 70$  MV/m due to the breakdown rate in the input and output couplers.

Most recently, it was found that pulsed heating in the input and output couplers may have been limiting the true performance of these test structures. Sharp edges in the coupler design were observed to have significant damage while the rest of the structures looked fine. Figure 5.9 is a photograph of one of these edges which shows damage that looks like melting of the copper although the expected temperature rise was relatively low.

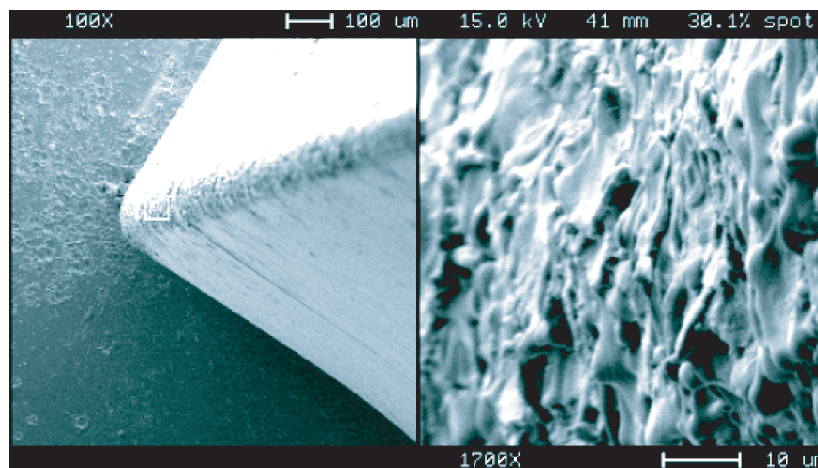


FIGURE 5.9. Scanning electron microscope photograph of damage along the sharp edge of an input coupler under two different magnifications.

The latest test structure was constructed with new input and output couplers. This structure was rapidly processed to 80 MV/m and then operated stably at 73 MV/m with a breakdown rate much less than required for JLC-X/NLC operation. It was subsequently processed up to 92 MV/m and has been operating at 90 MV/m with less than one breakdown event per day, a factor of 2 better than the JLC-X/NLC specification. The gradient performance of a number of the test structures is shown in Figure 5.10. Clearly, the latest structure, with the improved couplers, is performing well above the gradients desired for the JLC-X/NLC. Note, however, that the T-structures do not yet include the damping slots and manifolds.

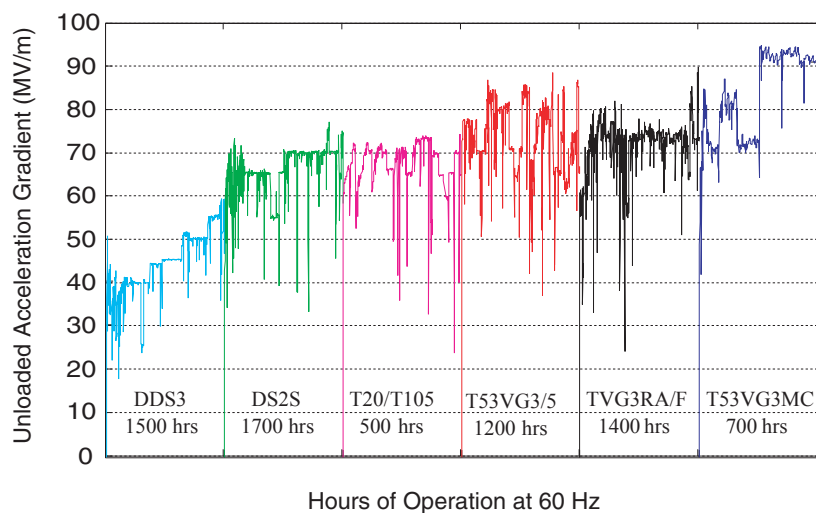


FIGURE 5.10. Gradients achieved in DDS3, a 1.8-m structure, and a number of test structures constructed from 2000 through 2002; note that most of the test structures exceeded the 70 MV/m goal and the most recent test structure, with a new design for the input and output couplers, is operating at 90 MV/m.

The structure testing for the gradient program has been done exclusively at NLCTA using the four accelerator slots in the two linac rf stations. To date, 12 structures have been tested in the two rf stations, which have been run in parallel for about 7000 hours at 60 Hz. As part of this testing, the SLED-II pulse compression systems have operated stably, producing up to 280 MW, 240 ns pulses. Although there have been klystron failures due to cracked windows and vacuum leaks, none have failed for more fundamental reasons (*e.g.*, chronic beam interception) after more than 30,000 hours of operation.

While the NLCTA essentially demonstrated an X-band rf system, construction of the facility began in 1993 when the rf components were still at an early stage of development. For example, the modulators that were built were of a line-type design, like the SLAC Linac modulators, with PFN's, thyratrons and transformers, rather than the current design which is based on solid-state switches. Similarly, the XL4 klystrons that were installed are solenoidal focused and not the periodic permanent magnet (PPM) focused tubes that are envisioned for the NLC. The SLED-II pulse compression system that was built was an improved version of the one initially tested to 200 MW in the SLAC Klystron Test Lab but is a single-moded design with components whose ultimate power handling capability is

probably more limited than that currently needed. Finally, the original accelerator structures were of the DS and DDS design that had been built to test long-range wakefield suppression methods but were limited to operating at  $\sim 40$  MV/m by rf breakdown and damage.

To test the present generation of X-band rf components, the NLC Test Accelerator is being upgraded. A solid-state modulator has been installed and will power four additional XL4 klystrons. These will feed a dual-mode SLED-II pulse compression system to produce roughly 600 MW in 400 ns by the middle of 2003; this is 30% greater than the present JLC-X/NLC specification. Finally, the rf power will be delivered to the NLCTA enclosure and will power 5.4 m of accelerator structure. In parallel, further testing of the PPM klystrons at KEK and SLAC will complete the demonstration of the JLC-X/NLC rf power source. During this period, the original NLCTA rf stations will continue to be used for high gradient testing. Full JLC-X/NLC prototype structures with the short-range and long-range wakefield control (HDDS1/HDDS2) will be tested in the middle of 2003 to verify the gradient performance.

### 5.3.2 Accelerator Structure SETup

The Accelerator Structure SETup (ASSET) is a facility dedicated to measuring the long-range transverse wakefield from an accelerator structure. The facility was constructed in 1995 and is located in Sector 2 of the SLAC linac. It uses the 1.19 GeV damped electron and positron beams from the SLC damping rings; the positron bunch comes first and excites the cavity, and the electron beam is then used to measure the resulting transverse wakefield. A chicane directs the positron beam to a dump, and the wakefield deflection of the electron beam can be detected using the  $\sim 30$  BPMs along Sector 2 which yield a resolution on the transverse wakefield measurements of roughly 0.1 V/pC/mm, more than sufficient for the JLC-X/NLC beam dynamics. The timing of the two beams can be adjusted so that the wakefield can be measured in the time domain, exactly as the bunch train would sample the wakefield, without resorting to a scan in frequency space that can miss high-Q resonances or the impact of higher frequency bands. A schematic of the facility is shown in Figure 5.11.

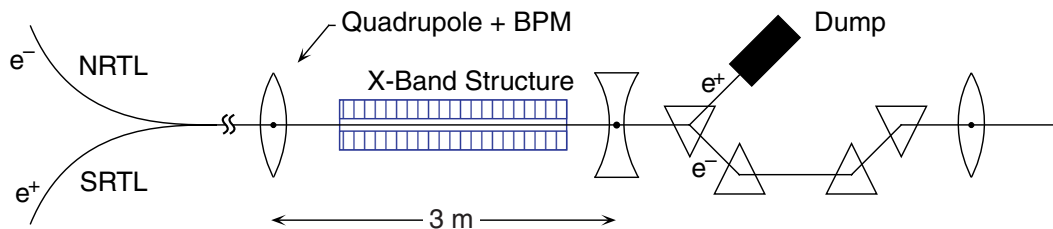


FIGURE 5.11. Schematic of the ASSET test facility.

The facility has been used to measure the wakefields in five JLC-X/NLC X-band accelerator structures as well as a JLC-C choke-mode structure from KEK and an X-band structure from CERN that was designed to study strong damping of the transverse wakefield as

proposed for CLIC. The accuracy of the measurements has been used to benchmark the wakefield calculation codes as illustrated in Figure 3.45 of the JLC-X/NLC Overview. The facility has also been used to verify the dipole-mode Beam Position Monitor (S-BPM) concept which would be used to align the X-band accelerator structures in the JLC-X/NLC linear collider. The resolution of the S-BPM is submicron and the accuracy appears to be similar.

The ASSET facility will continue to be used to measure the long-range wakefields of the JLC-X/NLC prototype structures. The next structure to be tested, the HDDS2, will be ready in mid-2003. This structure design will be tested in both the NLCTA to demonstrate the gradient performance as well as ASSET to verify the wakefields. In parallel, a dual-wire measurement is being developed as an alternate technique of directly measuring the transverse wakefield. This technique should prove to be much simpler and speedier to implement than mounting the structures in the ASSET facility and then measuring the wakefields using a beam. The ASSET facility will be used to benchmark this alternate approach.

### 5.3.3 Collimator Wakefield Test

To keep the background levels in the detectors manageable, the beam tails will have to be collimated with very high efficiency in all of the linear collider designs. Unfortunately, the transverse wakefields from any components that are placed close to the beam, such as a collimator, may amplify the beam jitter or dilute the beam emittance. There are few quantitative measurements of the collimator wakefields and it is difficult to model or calculate the high-frequency impedance due to a tapered planar collimator.

The collimator wakefield test facility is a dedicated facility that was designed to measure the short-range transverse wakefields induced by collimators or similar components that must be placed close to the beam. It is located in Sector 2 of the SLAC linac, close to the ASSET facility, and uses the damped 1.19 GeV beams from the electron damping ring. The apparatus consists of a large vacuum vessel roughly  $1.7 \times 0.6 \times 0.3$  m into which an insert with up to five collimator apertures is placed. The vessel and insert can be moved vertically in  $1 \mu\text{m}$  steps over a distance of  $\pm 1.5$  mm. The wakefield measurements are performed by moving the collimator and measuring the resulting deflection of the beam on  $\sim 30$  downstream BPMs. The resulting resolution of the transverse wakefield is better than  $0.1 \text{ V/pC/mm}$ . A photograph of the facility and a typical measurement are shown in Figure 5.12.

At this time, two inserts have been measured: a set of copper collimators to measure the geometric wakefields and benchmark the analytic approximations and a set of graphite collimators constructed at DESY. In 2003, it is planned to measure a set of collimators that will study the resistive wakefields and another set to study geometric wakefields in a regime that is closer to that expected in the JLC-X/NLC. Depending on the results, future studies can be scheduled as needed.

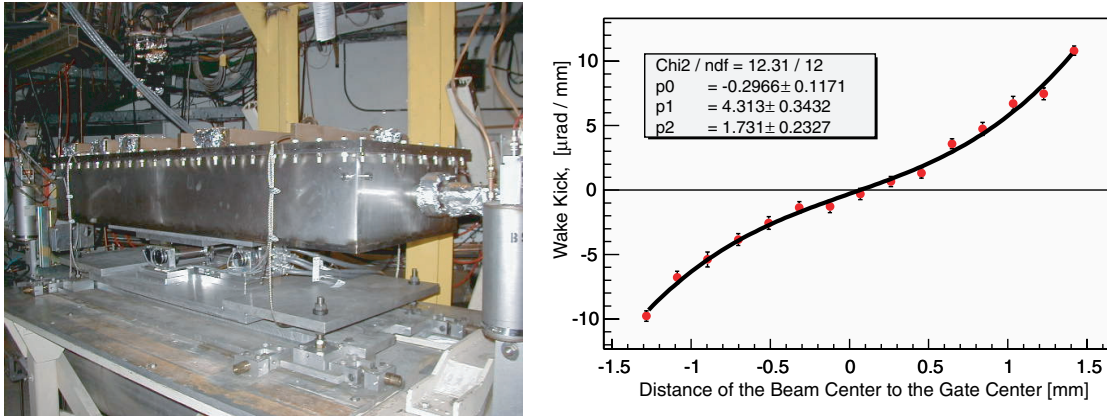


FIGURE 5.12. Photograph of the collimator wakefield test facility and an example of a measurement which also shows the nonlinearity of the wakefield when the beam is close to the collimator edges.

### 5.3.4 KEK Accelerator Test Facility

Aside from the SLAC/SLC, the ATF is the only linear collider R&D facility devoted to the production of low emittance beams, a critical challenge in LC beam dynamics and technology. The ATF is by far the largest of the linear collider test facilities, and includes a 1.5 GeV S-band injection linac, a  $\sim 130$  m circumference damping ring and an extraction line for beam analysis.

The ATF was built to demonstrate the feasibility of producing the low emittance beams required for a linear collider. As such, it has focused primarily on beam dynamics issues rather than technology. Experience from the SLC has shown that while technology is an important cost factor, beam dynamics, especially in the damping ring, can be a critical performance limitation. Technology development at ATF is centered on precision beam instrumentation, stabilization techniques and tuning methods.

The ATF international collaboration was formed in 1992 and initially included all major labs then involved in LC R&D. Construction was completed in 1997 and since then, the ATF has operated 20 weeks per year. Active members in the ATF collaboration include KEK, eight Japanese Universities, SLAC, LBNL, BINP and Tomsk.

The layout of the ATF is shown in Figure 5.13 while the design parameters are summarized in Table 5.2 and compared with what has actually been achieved. The emittances given are based on wire scanner measurements of the extracted beam, with the ring operating at 1.28 GeV in single bunch mode. The quoted errors are estimated from analysis of the fitted wire scanner data, combined with the observed statistical fluctuations of the measurements.

To achieve the low emittance goal, ATF operation has focused on six main areas of investigation: (1) tuning techniques and error correction, (2) single bunch collective effects (*e.g.*, intrabeam scattering), (3) wiggler performance, (4) damping ring acceptance, (5) extracted beam jitter, and (6) multibunch instabilities.

### ACCELERATOR TEST FACILITY FOR LC

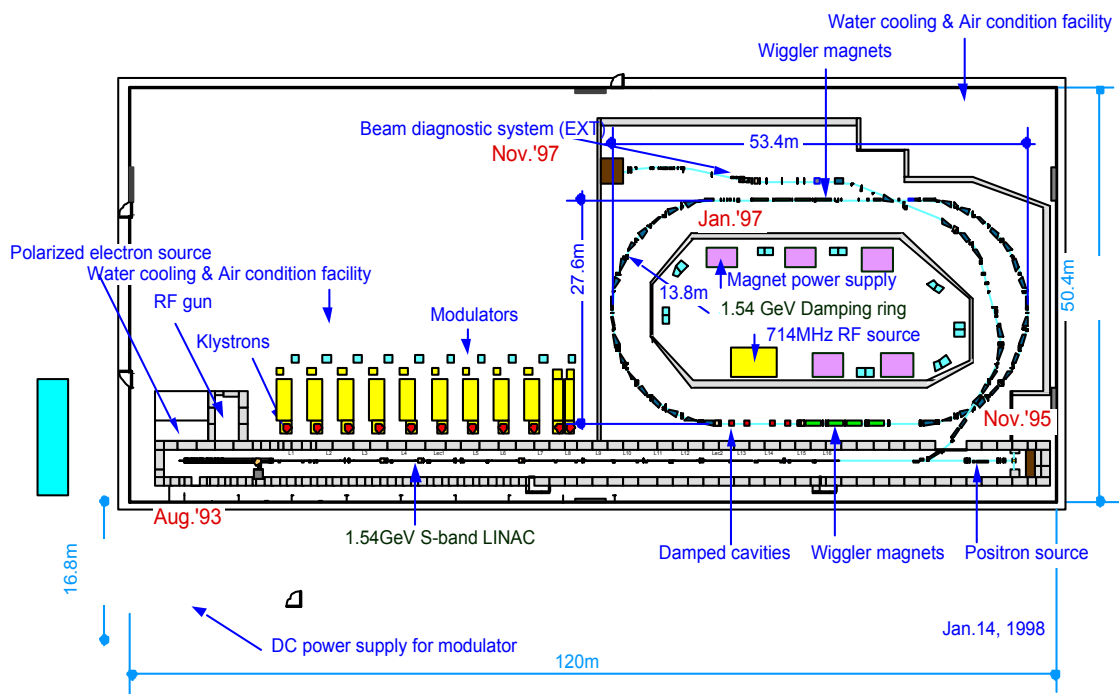


FIGURE 5.13. Layout of ATF.

TABLE 5.2

The design goals of the ATF and the accelerator performance achieved. The numbers in parenthesis indicate the number of particles per bunch for the particular measurement.

Items	Achieved Values	Design
<b>Linac status</b>		
Maximum beam energy [GeV]	1.42	1.54
Maximum gradient with beam [MeV/m]	28.7	30
Single bunch population	$1.7 \times 10^{10}$	$2 \times 10^{10}$
20 multibunch population	$7.6 \times 10^{10}$	$20 \times 10^{10}$
Energy spread (full width) [%]	<2.0 (90% beam)	<1.0 (90% beam)
<b>Damping ring status</b>		
Maximum beam energy [GeV]	1.28	1.54
Momentum compaction	0.00214	0.00214
Single bunch population	$1.2 \times 10^{10}$	$2 \times 10^{10}$
COD (peak to peak) [mm]	$x \sim 2, y \sim 1$	1
Bunch length [mm]	$\sim 6$	5
Energy spread [%]	0.08	0.08
Horizontal emittance [m·rad]	$(1.33 \pm 0.04) \times 10^{-9}$ ( $2 \times 10^9$ ) $(1.94 \pm 0.11) \times 10^{-9}$ ( $8 \times 10^9$ )	$1.4 \times 10^{-9}$
Vertical emittance [m·rad]	$(1.1 \pm 0.1) \times 10^{-11}$ ( $2 \times 10^9$ ) $(2.2 \pm 0.1) \times 10^{-11}$ ( $8 \times 10^9$ )	$1.0 \times 10^{-11}$
Multibunch population	$19 \times (0.6 \times 10^{10})$	$20 \times (1 \times 10^{10})$
Multibunch vertical emittance [m·rad]	$(2-3) \times 10^{-11}$	$1.0 \times 10^{-11}$

### 5.3.4.1 Emittance

The primary design goal of the ATF damping ring is to obtain a vertical normalized emittance less than  $3 \times 10^{-8}$  m-rad with a high intensity ( $0.7\text{--}3.0 \times 10^{10}$   $e^-$ /bunch) multibunch (10–40 bunches/train) beam. The ATF damping ring currently operates at 1.28 GeV beam energy at a repetition rate of 3.125 Hz with one bunch train of 20 bunches with 2.8 ns bunch spacing and  $0.1\text{--}1.0 \times 10^{10}$  particles/bunch. Extremely low emittance studies have been done in single bunch mode, resulting in the smallest single bunch, low current emittance recorded in the world,  $2.8 \times 10^{-8}$  m-rad (normalized).

The tuning procedure to obtain low emittance involves the successive application of steering, dispersion, and coupling corrections. Considerable work has been done to characterize the damping ring optics, resulting in high confidence in the present model. For instance, beam-based magnet field measurements (lattice diagnostics) uncovered quadrupole field-strength errors on the order of 1%. Correcting the optics model to account for these errors produced a model accurate to 0.01%. To correct residual alignment errors, beam-based alignment of focusing and sextupole magnets has begun. In late 2002, using new high-resolution ring BPMs, a quick, accurate beam-based alignment procedure has been developed to provide insight into the nature of the optics corrections that are presently used for emittance optimization. This should make it possible to identify sources of instability and quantify the physical limits on the minimum vertical emittance. This is one of the highest priority beam studies.

The contribution of the wiggler magnets to the damping time was found to be consistent with the design. However, they are not presently used because of a dynamic problem (the first field integral differs considerably from zero).

The transverse acceptance after tuning was found to be  $0.38 \times 10^{-6}$  m-rad, which is considerably smaller than the design specification of  $0.90 \times 10^{-6}$  m-rad ( $3\sigma$  of the assumed injected beam size) and also smaller than the simulation value from SAD of  $1.5 \times 10^{-6}$  m-rad ( $\Delta p/p = \pm 1.5\%$ ). However, the measured value is still more than  $3\sigma$  of the actual injected beam size (rms  $0.040 \times 10^{-6}$  m-rad).

During ATF construction, the floor was carefully engineered with 14 m deep concrete pilings in order to produce a mechanically stable platform for the ring. Nonetheless, early experience with the ring showed a sensitivity of the floor to thermal and seasonal drifts, especially in the circumference. Correction procedures have been developed.

With respect to intrabeam scattering, single bunch studies have shown a dependence of the measured emittance on both the bunch current and the longitudinal emittance, indicating strong intrabeam scattering (IBS). The results indicate a stronger effect than would be suggested by current IBS theory, and further study is needed. With the installation of an rf photocathode gun as described later, it will be possible to continue these IBS studies at higher current, with charge up to  $2 \times 10^{10}$   $e^-$ /bunch.

### 5.3.4.2 Extraction kicker

To stabilize extraction from the damping ring, the ATF has a double kicker system in the ring and extraction line which compensates for jitter in the kick angle due to the kicker magnet. This scheme has been shown to reduce the extracted beam fractional jitter to

$2.8 \times 10^{-4}$  in single bunch mode. The improvement due to the double kicker cancellation is at least a factor of 3.3. The multibunch performance of this system has not yet been verified, but this will be done when a multibunch BPM currently being developed becomes available.

### 5.3.4.3 R&D on Diagnostic Devices

Additional studies at ATF have been aimed at developing the technology required to accurately measure very small beams. There are five wire scanners in the extraction line, a laser-wire monitor in the ring, and Optical Transition and Diffraction Radiation (OTR and ODR) monitors under development in the extraction line.

The ATF **laser wire** closely resembles a design which is expected to be widely used in the LC. A laser beam with a very thin waist is generated in an optical cavity formed by nearly concentric mirrors. The laser intensity is amplified by adjusting the cavity length to meet the Fabry-Perot resonance condition. The cavity constructed for the ATF has produced a beam waist of  $12 \mu\text{m}$  ( $2\sigma$ ) and an effective power of 100 W, with good long-term stability. The laser wire is installed in the ring at a location with a transverse electron beam size of  $\sim 10 \mu\text{m}$ . It has been used over the last year to make accurate measurements of the vertical emittance of each bunch in the ring.

**Optical Transition Radiation profile monitors** are also expected to see widespread use in the LC in order to provide one-shot images of low emittance beams with a resolution well below typical beam sizes. The 2-D image produced by OTR is desirable in order to accurately determine  $x$ - $y$  and  $y$ - $z$  coupling and other phase space distortions. A monitor currently being tested has the resolution required for LC design parameters ( $2 \mu\text{m}$ ), well below the current state of the art for such monitors ( $20 \mu\text{m}$ ). To date, beam sizes of  $5 \mu\text{m}$  have been imaged and tests of transition radiation target longevity have been done.

A “proof-of-principle” experiment on the use of **Optical Diffraction Radiation** (ODR) as a single pulse beam profile monitor has been done using the electron beam extracted from the DR. Measurements have been made of the yield and the angular distributions of the optical diffraction radiation from a thin metal target at different wavelengths, impact parameters and beam characteristics.

### 5.3.4.4 Polarized Positron Production

Studies are underway at ATF to demonstrate a new method of generating highly polarized positrons through Compton scattering of polarized laser light off relativistic electron beams, where the photons produced are subsequently converted into pairs. A preliminary experiment was performed in the ATF extraction line in 2002, and a yield of  $1 \times 10^6$  polarized photons/pulse was measured.

### 5.3.4.5 Multibunch Operation

An early study for multibunch operation demonstrated a new technique for beam loading compensation in the injector linac, where two rf side-bands were applied to compensate for the bunch-by-bunch energy deviation due to beam loading.

In October 2002, the thermionic gun and buncher system were replaced by a Cs<sub>2</sub>Te cathode rf source in order to increase the injection efficiency into the ring to  $\sim 100\%$  and to improve performance during multibunch operation. This successfully doubled the stored charge in the ring ( $6 \times 10^9$ /bunch with 19 bunches), but the charge uniformity and stability is still poor due to the available laser and will be improved soon. The higher charge will allow more precise studies of single bunch intensity dependent phenomena such as intrabeam scattering, fast ion instability and impedance effects.

### 5.3.4.6 Future plans

The immediate ATF goals are understanding the minimum achievable single bunch emittance and obtaining stable operation with three 20 bunch trains. A program of theoretical and experimental studies has been planned that is focused on understanding the correction and optimization procedures, the stability of the ring component alignment, intrabeam scattering emittance growth and the multibunch beam dynamics mentioned before. Table 5.3 lists ATF historical milestones and plans.

TABLE 5.3  
ATF timeline and plans

Date	Milestone
1992	ATF Collaboration established
1993	Injector completed (80 MeV)
1995	Linac completed
1997	Ring and extraction transport completed
1998	Vertical emittance measurement using Touschek effect and high resolution synchrotron light interferometer
2000	Vertical emittance minimization using wire scanners and intrabeam scattering results
2001	Photocathode gun tests showing excellent transmission
2001	Instrumentation achievements: ring laser wire, high precision OTR, multibunch BPMs and X-ray SR beamline
2002	Photocathode gun installation and BPM upgrade for beam-based alignment
2003	Beam-based alignment
2003	Multibunch instability studies
2004	3 pm-rad single vertical emittance ( $0.75 \times 10^{-8}$ m-rad normalized)
2004	High intensity multibunch operation ( $1 \times 10^{10}$ $e^-$ in each of 20 bunches)

### 5.3.5 Final Focus Test Beam

The Final Focus Test Beam (FFTB) at SLAC was constructed during the early 1990s by an international collaboration that included most of the laboratories interested in linear colliders at that time. The primary goal of the facility was to focus the low emittance 50 GeV SLAC electron beam down to a spot of  $1\ \mu\text{m}$  by  $60\ \text{nm}$  with beta functions of  $\beta_x^* = 3\ \text{mm}$  and  $\beta_y^* = 100\ \mu\text{m}$ . This was to demonstrate the optical demagnification that would be required in a future linear collider. A secondary goal of the experiment was to develop and demonstrate some of the high resolution diagnostics, controls, and tuning schemes that would be required in a future collider.

To achieve the small spot sizes, the final focus system is roughly 180 m long with another 180 m of beam line that transports the low emittance beam from the SLAC switchyard to the final focus proper. From the beginning, the FFTB contained 34 quadrupole magnets, 14 dipoles, and 8 sextupoles. The optics was chromatically corrected to third-order by placing the correction sextupoles in pairs, separated by a  $-I$  transform, and not interleaving the horizontal and vertical chromaticity corrections. This is quite similar to the correction schemes presently proposed for the future linear colliders.

Each of the quadrupole and sextupole magnets was installed on a remote-controlled magnet mover which had a range of  $\pm 1.5\ \text{mm}$  horizontal and vertical motion and  $\pm 5\ \text{mrad}$  rotation about the beam axis, and a step size that was  $0.3\ \mu\text{m}$  and  $1\ \mu\text{rad}$ , respectively. These magnet movers reduced the need for dipole correctors, and very few correctors were installed. In addition, high resolution BPMs were mounted in the bore of each quadrupole; these BPMs were measured to have pulse-to-pulse resolutions that were  $1\ \mu\text{m}$  and drifts of less than  $3\ \mu\text{m}$  per week. A set of three 5.7 GHz rf BPMs were also installed at the nearest upstream vertical image of the IP where the nominal beam size was  $500\ \text{nm}$ ; these BPMs were measured to have a resolution of  $30\ \text{nm}$ . Finally, wire scanners with wire diameters of  $3.8\ \mu\text{m}$  were installed and used to measure beam sizes of  $0.7 \pm 0.1\ \mu\text{m}$  with aspect ratios of 200:1. All of these diagnostic and control devices demonstrated performance close to what will be needed in a future linear collider. Figure 5.14 shows a schematic of a magnet mover and the reconstructed beam trajectories through the three rf BPMs along with the BPM resolution that can be extracted from the three simultaneous measurements.

The FFTB ran six times between 1993 and 1997 with periods that ranged from a few days to almost two weeks. During the runs, beam-based alignment would be used to align the quadrupoles and sextupoles and verify the quad-to-BPM offsets. The linear optics would then be tuned and finally the nonlinear optical elements would be adjusted to achieve the small spot sizes. The left side of Figure 5.15 shows a histogram of the measured vertical spot size from the December 1997 run. The measured spot size was  $70 \pm 7\ \text{nm}$ , and was stable over a 48 hour period. The expected spot size at this time was  $59 \pm 8\ \text{nm}$ , including contributions from both the actual rms size of the beam and the rms beam jitter at the focal point, which was measured to be approximately  $35\ \text{nm}$ ; the expected spot size is shown in Figure 5.15 by the red bar above the histogram. Similar results had been measured during previous runs. The right side of Figure 5.15 shows the signal from the Shintake Laser-Interferometer IP beam size diagnostic during the December 1994 run. The beam size is measured with Shintake monitor by detecting the Compton scattered electrons while scanning the beam across the interference fringes generated by crossing two laser beams at a small angle. This device has a beam size resolution of roughly  $40\ \text{nm}$ .

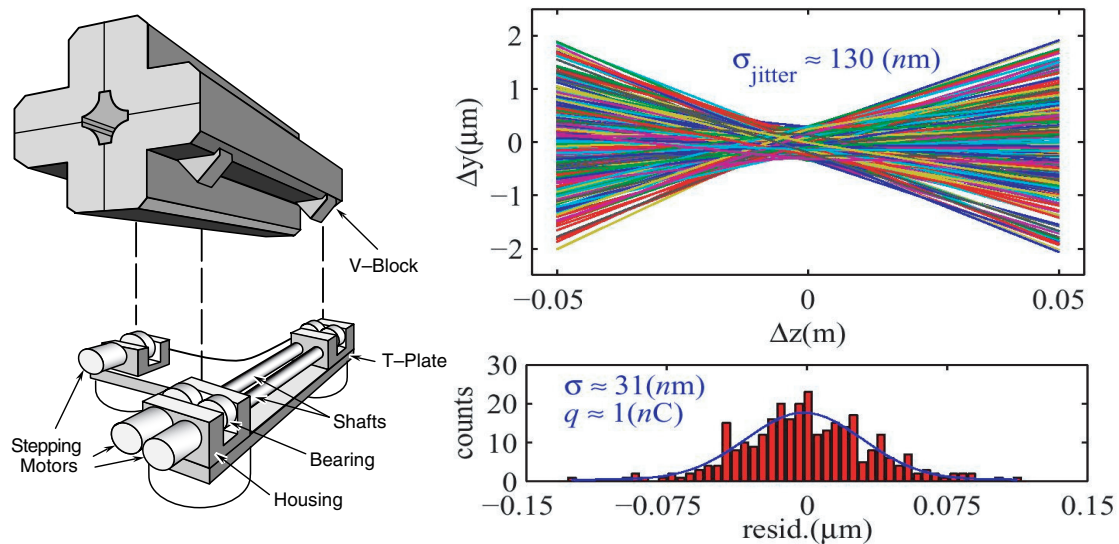


FIGURE 5.14. Examples of diagnostics and controls developed for the FFTB: (left) schematic of a remote magnet mover with 300 nm steps in X and Y and (right) measured beam trajectories through an rf BPM triplet having  $\sim 30$  nm resolution showing 130 nm of beam jitter.

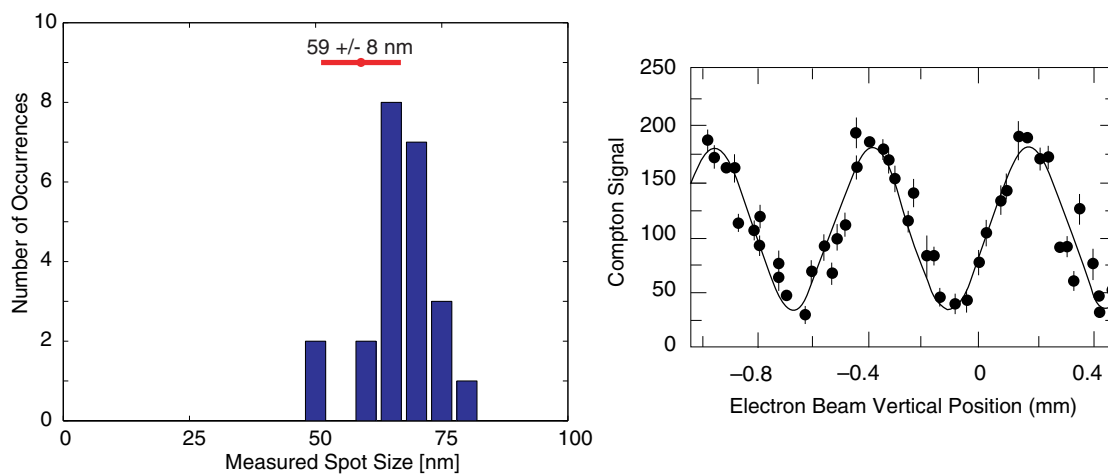


FIGURE 5.15. Histogram of the FFTB vertical spot size measurements (left) with an average of  $70 \pm 7$  nm versus the expected size of  $59 \pm 8$  nm and (right) a plot showing a typical measurement using the Shintake laser interferometer corresponding to a 77 nm beam spot.

## TEST FACILITIES AND OTHER PROJECT R&D PROGRAMS

Most of the magnets were installed on vibration-damped Anocast stands and there appears to be little amplification of the natural ground motion by the support, mounting, or mover system. In addition, measurements comparing the motion with and without coolant flow show a difference of only 2–3 nanometers. Because they were significantly larger and heavier, the final doublet magnets were mounted on a special table with a separate mover system. Subsequent vibration measurements showed that the table was moving by about 40 nm. This is consistent with independent measurements of the motion of the beam relative to the IP beam size diagnostic.

In summary, the FFTB project demonstrated that the optical demagnification required by the linear collider designs is possible to achieve and maintain. The project also developed and then demonstrated much of the diagnostic and control hardware that will be needed in a future linear collider including the high-resolution beam position monitors, beam size monitors, and magnet movers. Finally, many of the tuning and beam-based alignment techniques that will be needed were demonstrated giving additional confidence in the linear collider designs. At this time, the FFTB enclosure is being utilized for other purposes and there are no plans to revive the beam line as a final focus system.

### 5.3.6 Stabilization Demonstrations

The stabilization demonstrations involve work on four different fronts. First, extensive vibration and drift measurements have been made around the world to understand the natural levels of motion. In particular, fast ground motion (relevant for collision stability) has been measured at many laboratories as well as the potential NLC sites in California and Illinois and many of the JLC sites in Japan; the spectra from some of these measurements can be seen in Figure 3.52 of the JLC-X/NLC Overview. Most of the sites considered thus far are sufficiently quiet that there is a significant margin for additional cultural noise. In addition, to understand the tolerances on the cultural noise, transmission measurements from either the surface to the tunnel or between two twin tunnels are being carried out or will be made in 2003. Results of these studies will guide the design of passive vibration protection for the vibration producing equipment. Similarly, the slow motion (relevant for emittance preservation) has been studied extensively at FNAL, SLAC and locations in Japan. These sites are expected to have tolerable slow ground motion, as confirmed either by direct measurements or by comparison with geologically similar sites. As part of the investigation of the slow ground motion a new hydrostatic level system has been developed with submicron resolution. Such a system may also be used as part of the alignment system for a future linear collider.

Second, the effect of cultural vibration sources on the stability of the linac quadrupoles has been studied because, although the jitter tolerances are relatively loose at 10 nm, there are thousands of magnets that require this level of stability. The feasibility of such stability has been demonstrated in several earlier independent measurements, such as those at the FFTB; however in the linacs there may be additional sources of noise. Presently, SLAC and FNAL are studying the vibration transmitted to the quadrupoles from rf structures, which may have large vibration due to the flow of cooling water. Preliminary tests, which used a simplified model of the linac rf girder, showed  $\sim 300$  nm of motion on the rf structure but little coupling of the structure to the quadrupole and confirmed the feasibility of achieving

the required quadrupole stability. Design of a full linac girder prototype is ongoing and will be done with consideration of the stability requirements.

Next, the final doublet magnets, that focus the beams down to the very small spot sizes at the IP, have tolerances of roughly 1 nm, a factor of 10 tighter than most of the other quadrupoles. Furthermore, the supports for these magnets are complicated because the magnets are, at least partially, located inside the high-energy physics detector. For these reasons, it is thought that some active stabilization system will be required for these magnets. Although commercial systems are available that can achieve the required stability, they are not well adapted to the details of the interaction region where an extended object must be stabilized in a very compact region with strong magnetic fields. To this end, a program at SLAC has used inertial sensors and electrostatic actuators to stabilize a 100 kg block in six degrees-of-freedom and is developing compact, nonmagnetic, high performance sensors; these are shown in Figure 5.16. In 2003, this inertial system will be used to stabilize an extended object that more closely represents a final quadrupole magnet, and then the system will be demonstrated in an environment that approximates the real interaction region. In parallel, an “optical anchor,” where optical interferometers are used to rigidly anchor an object to an accurate reference, is being studied at the University of British Columbia. This system has the advantage of having better low frequency ( $f < 1$  Hz) performance than the inertial systems but must be based on a very stable reference. It is likely that the final system will involve a combination of inertial stabilization and optical anchors.

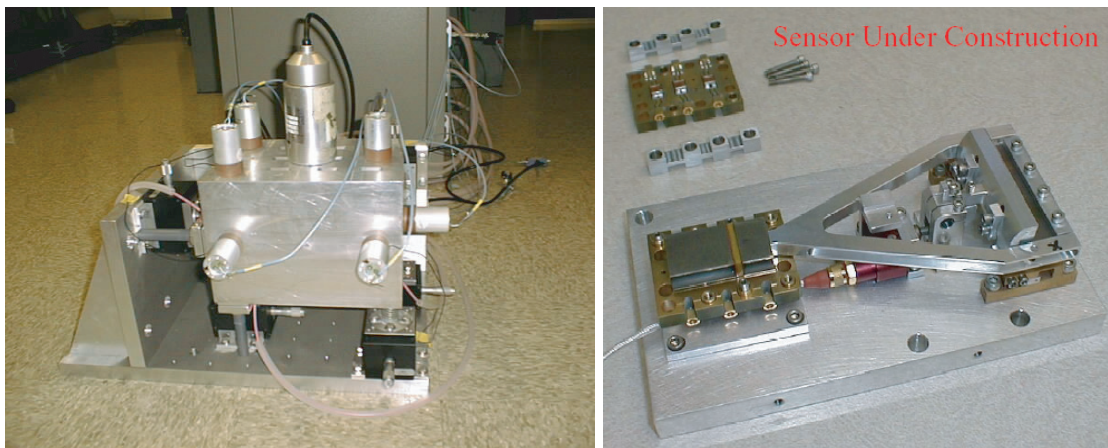


FIGURE 5.16. Photograph (left) of 100 kg block stabilized in six degrees-of-freedom and (right) of the compact nonmagnetic inertial sensor under development.

Finally, a fast intra-train feedback system is being developed to further ensure the stability of the beam at the IP. This feedback system must operate extremely rapidly because the full JLC-X/NLC bunch train is only 270 ns long. Presently, groups from Queen Mary College in London and Oxford University are working on FONT, Feedback On Nanosecond Timescales. This facility uses the NLCTA beam to simulate the beam entering and exiting the IP as illustrated in Figure 5.17. Tests have shown that FONT is able to reduce the

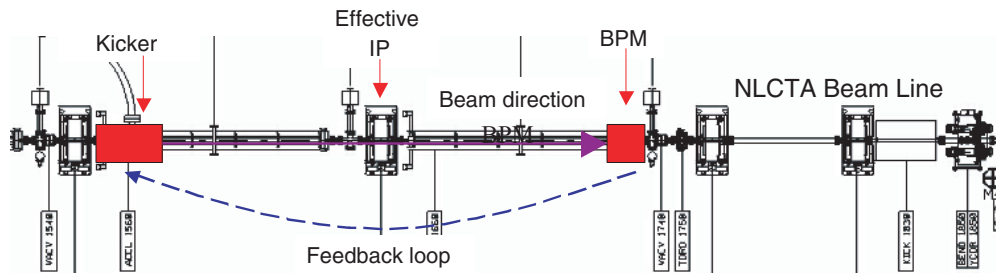


FIGURE 5.17. Schematic of the FONT experiment in the NLC Test Accelerator.

amplitude of an induced oscillation by roughly a factor of 10 with a latency of  $\sim 60$  ns. In 2003, new kicker power supplies and improved feedback electronics will be tested with the NLCTA beam to demonstrate improved latency times.

## 5.4 CLIC

### 5.4.1 The Test Facility CTF3 Under Construction

#### 5.4.1.1 Introduction

The CLIC design relies on electron acceleration with high gradients of 150 MV/m at 30 GHz with rf pulse length of 130 ns. The rf power requirement is 460 MW per meter of linac length. Therefore a very efficient and reliable source of rf power is required. The scheme is based on a drive beam running parallel to the main beam, whose bunch structure carries a 30 GHz component. The rf power is extracted from the drive beam in Power Extraction and Transfer Structures (PETS) and transferred to the main beam [1].

The required drive beam time structure is produced by compressing a long bunch train with low bunch repetition frequency, which is accelerated with low rf frequency. Subsequent packets of this bunch train are interleaved in isochronous rings, which thereby increase the bunch repetition frequency and the peak current in these packets. Power efficiency being of utmost importance for CLIC, the drive beam with high peak current is accelerated in fully beam-loaded low-frequency cavities, so that the power, except for wall losses, is completely converted to beam energy. New accelerator structures are required with very strong damping of beam induced Higher Order Modes (HOM) to keep the bunch trains stable.

The main goal of CTF3 is to demonstrate the key concepts of the new rf power generation scheme, namely the bunch compression scheme and the fully loaded accelerator operation. The drive beam pulse obtained after compression (140 ns, 35 A) will be sent to special resonant structures to produce 30 GHz rf power with the nominal CLIC parameters, to test accelerating cavities and waveguide components.

The facility [2] will be built in the existing infrastructure of the LPI (LEP-Pre-Injector) complex and will make maximum use of equipment which became available after the end of LEP operation. In particular, the existing rf power plant from LIL at 3 GHz and most of

the magnets will be used. The project is based in the CERN PS Division with collaboration from many other Divisions at CERN, as well as from INFN Frascati, SLAC, IN2P3/LAL at Orsay, Rutherford Appleton Laboratory (RAL) and the University of Uppsala.

A “probe beam” simulating the CLIC main beam will be available to demonstrate acceleration with the 30 GHz equipment at the CLIC design accelerating gradient. An intermediate test station is foreseen immediately after the linac for power-testing CLIC components at longer pulse length than presently available at CTF2 at the earliest possible moment.

The final configuration of CTF3 is shown in Figure 5.18 and the main systems of CTF3 are described here. The schedule planned for CTF3 is indicated in the Figure 5.19.

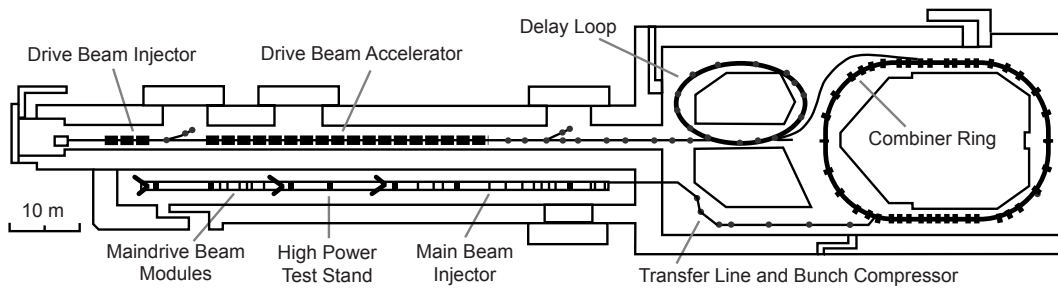


FIGURE 5.18. Layout of the final configuration of CTF3.

Task Name	2002				2003				2004				2005				2006				
	Q3	Q4	Q1	Q2	Q3																
<b>CTF2</b>	▬																				
<b>CTF3 - Preliminary Phase</b>	▬																				
<b>INITIAL PHASE</b>	▬																				
Injector Initial Phase	▬																				
Drive Beam Accelerator	▬																				
End of Linac Test-stand	▬																				
Combiner Ring	▬																				
Commissioning Initial Phase	▬																				
<b>NOMINAL PHASE</b>	▬																				
Shielding + CE	▬																				
Delay Loop	▬																				
Injector Modification	▬																				
RF Power 1.5 GHz	▬																				
Commissioning Nominal Phase	▬																				
CLEX	▬																				

FIGURE 5.19. Chart with CTF3 schedule.

### 5.4.1.2 Drive Beam Injector

The drive beam injector [3] is built in collaboration with SLAC (providing the gun triode and the beam dynamics design) and LAL/Orsay (providing the gun electronics circuitry and the 3 GHz pre-bunchers).

The 1.6  $\mu\text{s}$  long drive beam pulse is generated by a 140 kV, 9 A thermionic triode gun. The gun is followed by a bunching system composed of a set of 1.5 GHz subharmonic bunchers, a 3 GHz pre-buncher and a 3 GHz tapered-velocity traveling-wave buncher. The phase of the subharmonic bunchers is switched rapidly by 180 every 140 ns. In order to obtain a fast switching time ( $\leq 4$  ns), the 1.5 GHz rf source must have a broad bandwidth (about 10%) and a peak power of 500 kW [4]. The bunches thus obtained are spaced by 20 cm (two 3 GHz buckets) and have a charge of 2.3 nC each, corresponding to an average current of 3.5 A. As a result of the phase switching, the drive beam pulse is composed of 140 ns subpulses, which are phase-coded and can be separated later by transverse deflectors working at 1.5 GHz.

The injector is completed by two 3 GHz traveling-wave structures, bringing the beam energy up to about 20 MeV. Solenoidal focusing with a maximum on-axis field of 0.2 T is used all along. A magnetic chicane with collimators downstream of the injector will eliminate the low energy beam tails produced by the bunching process. The chicane region will also be instrumented to perform beam-size and energy-spectrum measurements. An alternative option to the thermionic injector scheme, based on the use of an rf photoinjector, is also under study as a potential later upgrade [5].

### 5.4.1.3 Drive Beam Accelerator

The drive beam pulse is brought to its final energy (150 MeV) in the drive beam accelerator, composed of 8 modules of 4.5 m length. Each module consists of two accelerator structures, identical to the ones used in the injector, a beam position monitor, a quadrupole triplet and a pair of steering magnets. Beam simulations have shown that the initial value of the normalized rms emittance (100  $\mu\text{m}\cdot\text{rad}$ ) is conserved during acceleration despite the high beam current and the long beam pulse, provided that the transverse Higher Order Modes (HOMs) are suppressed. The traveling-wave structures work in the  $2\pi/3$  mode, have an active length of 1.13 m with a filling time of 100 ns and operate at a loaded gradient (nominal beam current) of about 8 MV/m, with an rf-to-beam efficiency of 92% approximately. The structure (called SICA, for Slotted Iris Constant Aperture) uses four radial slots in the iris to couple the HOMs to SiC loads (see Figure 5.20). The selection of the modes coupled to the loads is determined by their field distribution, so that all dipole modes are damped. The  $Q$ -value of the first dipole is reduced to about 5. The HOM frequency detuning is obtained by nose cones of variable geometry. The aperture can therefore be kept constant at 34 mm, yielding a small amplitude of the short-range wakefield. A SICA test prototype is under construction. The rf power is supplied by eight 30 MW klystrons and compressed by a factor of 2 to give a peak power at each structure input of about 30 MW. The pulse compression system is based on the existing LIPS system; however, a programmed phase ramp is used to get an almost rectangular rf pulse [6] with the required phase stability. New cavities to complement and partly replace the existing storage cavities, the BOC (Barrel Open Cavities) are presently under development.

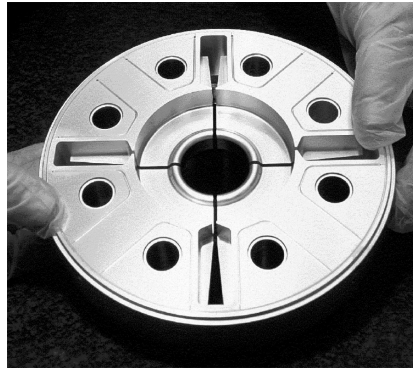


FIGURE 5.20. Prototype cell for the SICA structure.

#### 5.4.1.4 Delay Loop and Combiner Ring

After the linac, a first stage of electron pulse compression and bunch frequency multiplication of the drive beam is obtained using a transverse rf deflector at 1.5 GHz and a 42 m long delay loop. The phase-coded 140 ns long subpulses are first separated and then recombined by the deflector after half of them have been delayed in the loop. The beam is then a sequence of five 140 ns long pulses with twice the initial current, separated by 140 ns “holes” (see Figure 5.21). An 84 m long combiner ring is then used for a further stage of pulse compression and frequency multiplication by a factor of 5, through injection with 3 GHz transverse rf deflectors [2].

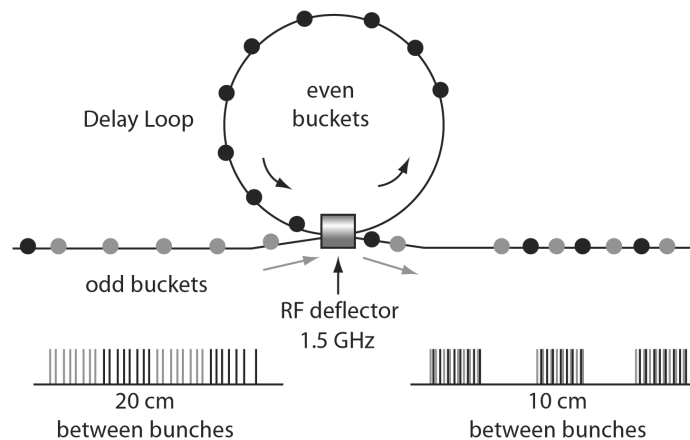


FIGURE 5.21. Schematic description of the pulse compression and frequency multiplication using a delay loop and a transverse rf deflector. Note that the last bunch coming from the left is in an even bucket again for consecutive deflection into the delay loop, therefore shifted in phase. After the delay loop, there are 140 ns between the trains. After the combiner ring, a single 140 ns long drive beam pulse with a current of 35 A is obtained. The final bunch spacing is 2 cm.

## TEST FACILITIES AND OTHER PROJECT R&D PROGRAMS

The design of the delay loop, the combiner ring and the related beam lines is under the responsibility of INFN/Frascati [7]. Both the delay loop and the ring must be isochronous in order to preserve the short bunch length required. The combiner ring consists of four isochronous arcs, two short straight sections and two long straight sections for injection and extraction. The ring arcs are triple-bend achromats, with negative dispersion in the central dipole. A precise tuning of the momentum compaction value can be obtained by a variation of the magnetic strength of the central quadrupole in each arc. Three sextupole families in the arcs provide a cancellation of the second-order momentum compaction, while controlling both the horizontal and vertical chromaticities. Two wiggler magnets are foreseen in order to adjust the ring circumference precisely to a  $N+1/5$  multiple of the bunch spacing (with a total adjustment range of  $\pm 1$  mm), and are placed in the short straight sections (one similar wiggler is located in the delay loop). Prototypes of these wigglers are under construction. The injection and extraction regions of the ring, with similar requirements, have identical lattices. Injection and extraction septa are placed symmetrically in the center of the long straight sections. The  $\pi$  betatron phase advance between the two ring-injection deflectors is obtained by four quadrupoles arranged symmetrically around the septum. In the extraction region this assures the required  $\pi/2$  phase advance between the extraction kicker and the septum.

A potential problem of the combination process with a high bunch charge is the effect of multibunch beam loading on the fundamental mode of the deflecting cavities. Detailed studies of the effect have been made [8], showing that the transverse beam stability can be sufficiently improved by a proper choice of the deflector parameters, of the  $\beta$ -function at injection and of the ring tune. The results are summarized in Figure 5.22 for position errors  $\Delta x$  and angle errors  $\Delta x'$ .

The use of short, high-charge bunches puts severe requirements on the ring impedance and makes coherent synchrotron emission a serious issue. The main effects are beam energy loss and energy spread increase.

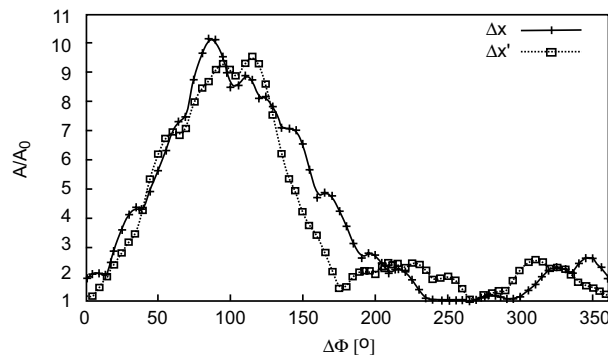


FIGURE 5.22. Amplification of an initial error in position  $\Delta x$  (crosses) and angle  $\Delta x'$  (squares) of the injected beam as a function of the betatron phase advance in the ring, after five turns. The ring tune has been chosen in the low amplification region, close to a phase advance of  $260^\circ$ .

In order to minimize these effects, the rms bunch length can be increased from its value of 1.3 mm in the linac to a maximum of 2.5 mm in the delay loop and ring, by a magnetic chicane placed at the end of the linac. After combination, the individual bunches are then compressed in length to about 0.5 mm rms in a magnetic bunch compressor. The drive beam pulse is then transported to the 30 GHz test area.

#### 5.4.1.5 Main Beam and 30 GHz Test Area

A single 30 GHz decelerating structure, optimized for maximum power production, will be used in a high power test-stand where CLIC prototype accelerator structures and rf components can be tested at nominal power and beyond. Alternatively, the drive beam can be used in a string of decelerating structures to power a representative section of the CLIC main linac and to accelerate a probe beam. The probe beam is generated in a 3 GHz rf photoinjector and pre-accelerated above 100 MeV using 3 GHz accelerator structures recuperated from LIL. It can be accelerated further to about 500 MeV in 30 GHz CLIC accelerator structures powered by the drive beam, operated at a maximum gradient of 150 MV/m. This setup will allow to simulate realistic operating conditions for the main building blocks of the CLIC linac.

### 5.4.2 Development of the CLIC Accelerator Structures

CLIC presently runs a program of high-power structure tests using CTF2 as a power source. CTF2 [9] provides 30 GHz rf pulses of up to 280 MW with a pulse-length variable from 3 to 15 ns. This pulse length is larger than the fill-time of the structures built so far, but is short compared to the nominal 130 ns pulse-length of CLIC. Since the available power level exceeds by far the power needed for structure testing, a relatively simple pulse-stretching device could be envisaged in order to increase the pulse length in CTF2 up to 30 ns. Such a device has been made operational in CTF2 so that tests with longer pulses could be done before the dismantling of CTF2 planned in the autumn of 2002. Tests with a copper structure with reduced aperture achieved the same average gradient of 105 MV/m with either 15 or 30 ns pulse length.

The test facility CTF3 under construction and described previously will allow to produce 30 GHz rf power pulses of nominal length. Some 30 GHz structure testing with this new source will start in late 2004. Another experiment is in preparation at JINR/Dubna which will test pulsed heating limitations in 30 GHz cavities using a FEL as 30 GHz power source.

The program of structure tests is based on results obtained during the last ten years. The feasibility of reaching a gradient of 150 MV/m using the CLIC technology was demonstrated at SLAC and KEK with a small aperture X-band structure [10]. In CTF2, the constant impedance copper structures tested have reached mean accelerating gradients of 72 MV/m for a surface field of 317 MV/m. At these field levels, considerable surface damage is observed on the first iris, which connects the input coupler cell with the first regular cell and is exposed by far to the highest surface field. No significant damage is seen in the downstream cells. The damage pattern follows the field distribution. Structure rf conditioning to reach the damage level takes  $\sim 3 \times 10^5$  rf pulses. An experiment was then performed where an iris made of tungsten replaced the damaged region. Although the structure was powered for  $5 \times 10^5$  pulses to the same field levels as before, no damage

occurred on the tungsten iris. A short pulse experiment has been performed using a 3 ns long pulse on a structure with standard copper irises applying a 160 MV/m gradient for  $5 \times 10^5$  pulses. The pulse energy was the same as in the 72 MV/m and 15 ns run, but no damage occurred.

High power structure tests have been carried out during 2002 with reduced  $E_{surf}/E_{acc}$  ratio in the cells and in the coupler. Structures have been built with this end in view. The first structure already tested has an  $a/\lambda$  of 1.75, a phase advance  $2\pi/3$ ,  $E_{surf}/E_{acc}=2.2$  and  $v_g=0.046c$ . The couplers are of the mode launcher type. The surface field of the coupler nowhere exceeds the field of the regular cells and all the irises are made of tungsten with copper rings clamped in between. Very recent measurements showed that accelerating fields of 125 MV/m in average and of 152 MV/m in the first cell, corresponding to a peak surface field is 340 MV/m, were obtained in this structure, after 1.5 million rf pulses and without damage. They also indicate that the mode-launcher type power coupler overcomes the field limitations encountered with the couplers used so far.

The second structure has the same cell geometry, but is entirely made from OFHC copper and assembled by braze/diffusion bond at 820°C in vacuum. It reached an average accelerating field of 102 MV/m with a peak accelerating field in the first cell of 114 MV/m and a peak surface field of 255 MV/m. This structure showed signs of surface damage on the first regular iris, where the surface E-field is highest. The third structure, with molybdenum irises, was conditioned to an average accelerating gradient of 150 MV/m, with a peak accelerating field in the first cell of 193 MV/m and a peak surface field of 432 MV/m. No damage was observed. Comparing results from these structures will allow distinguishing material from geometry effects. A second set of structures (one tungsten/copper, one copper only) will be built using a phase advance of  $\pi/2$  with  $a/\lambda=2$ ,  $E_{surf}/E_{acc}=2$  and  $v_g=0.083c$ . These structures have a higher  $v_g$  than the first ones. High power tests of both sets and structure comparison will allow distinguishing effects due to surface field and to group velocity.

### 5.4.3 Study of the Magnet Vibration Stabilization

The magnet vibration tolerances for frequencies above approximately 4 Hz are severe in CLIC, of the order of 14 nm (4 nm) horizontally and 1.3 nm (0.2 nm) vertically, in the linacs (and in the final focus respectively). The most challenging requirements are in the vertical plane. Tolerances for uncorrelated rms vibration above 4 Hz are 1.3 nm for all the linac quadrupoles and 0.2 nm for the final doublet. It must be determined early whether these tolerances are feasible. A CLIC study on magnet stability and time-dependent luminosity was proposed in 2000 [11] to address this critical issue and the goal was stated as: "Show that the present design parameters of CLIC are feasible in a real accelerator environment, using and further developing latest cutting-edge stabilization technology and time-dependent simulation programs."

The study started after it was approved and funded in January 2001. Major steps have been taken in order to address the stated challenge:

- Vibration measurements with sub-nm resolution and accuracy were demonstrated in the frequency range of interest ( $>2$  Hz). Four identical vibration sensors were acquired.

- A test-stand for magnet vibration measurements was set up at CERN in the immediate neighborhood of roads, operating accelerators, manual shops, and regular office space.
- Available industrial solutions for vibration damping were reviewed and two state of the art systems were acquired. One system employs an active piezoelectric feedback on ground vibration (STACIS2000 from TMC). The other system (PEPS-VX from TMC) is an air-pressurized solution, offering passive damping, a micrometer alignment slow feedback, and a faster active feedback on table top motion.
- A table with a minimal structural resonance above 230 Hz was acquired to provide a stiff support of prototype magnets.
- A cooling water system (from tap water) was installed to test magnet vibration with cooling water flow.
- Also relying on active collaborations with DESY and SLAC colleagues, advanced simulation tools were set up.

The experimental work on stabilizing existing CLIC prototype magnets has started in April 2002. Results with the STACIS2000 system show that the system damps the floor vibration by about a factor of 20. Using this system, CLIC quadrupoles have been stabilized vertically to an rms motion of  $(0.9 \pm 0.1)$  nm above 4 Hz (see Figure 5.23), or  $(1.3 \pm 0.2)$  nm with a nominal flow of cooling water. For the horizontal and longitudinal directions respectively, a CLIC quadrupole was stabilized to  $(0.4 \pm 0.1)$  nm and  $(3.2 \pm 0.4)$  nm [12]. It is noted that the measured vibration levels in principle meet the requirements for the CLIC linac quadrupoles. An improvement by about a factor of 5 is required for the two final quadrupoles in the vertical direction.

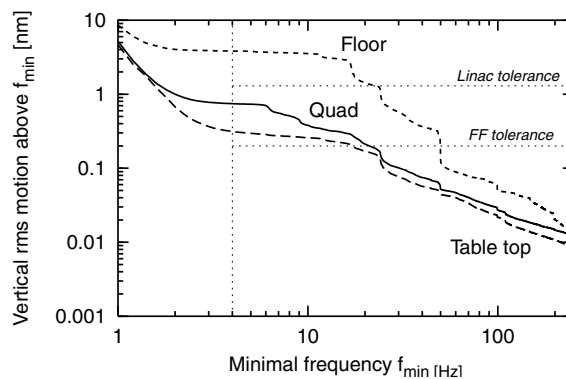


FIGURE 5.23. Vertical rms amplitude of vibration, integrated from above a given frequency  $f_{min}$ , versus this frequency. Vibration was simultaneously measured on the floor, on the quadrupole, and on the tabletop.

## TEST FACILITIES AND OTHER PROJECT R&D PROGRAMS

Future studies will aim at further reducing vibration levels, studying alignment stability, measuring structural resonances in magnets and supports, exploring environmental effects (*e.g.*, more studies on cooling water, magnetic fields, and so on), employing an alternative pneumatic system, and using the measurements for predictions of the CLIC luminosity stability. In addition, work will also aim at establishing a firm basis for a CLIC specific engineering solution that in principle could be based on or could include the tested technology.

# BIBLIOGRAPHY for CHAPTER 5

- [1] R. Corsini (ed.) and 15 co-authors, “The CLIC RF Power Source - A Novel Scheme of Two-Beam Acceleration for e Linear Colliders,” CERN 99-06 (1999).
- [2] R. Corsini, A. Ferrari, L. Rinolfi, T. Risselada, P. Royer, F. Tecker, “CTF3 Design Report,” Edited by G. Geschonke (CERN) and A. Ghigo (INFN), CERN/PS 2002-008(RF) and LNF-02/008(IR), (2002).
- [3] H. Braun and 6 co-authors, “An Injector for the CLIC Test Facility (CTF3),” CERN/PS 2000-052, Proc. of the XX Linac Conference, August 21–25, 2000, Monterey, USA.
- [4] G. Phillips, “A 500 kW L-Band Klystron with Broad Bandwidth for Sub-Harmonic Bunching in the CLIC Test Facility,” Proc. of the 5th Modulator-Klystron Workshop for Future Linear Colliders, April 26–27, 2001, Geneva, Switzerland.
- [5] I.N. Ross, “Feasibility Study for a CERN CLIC Photo-Injector Laser System,” CLIC Note 462 (2000).
- [6] I. Syratchev, “RF Pulse Compressor Systems for CTF3,” Proc. of the 5th Modulator-Klystron Workshop for Future Linear Colliders, April 26–27, 2001, Geneva, Switzerland.
- [7] C. Biscari and 12 co-authors, “CTF3 - Design of Driving Beam Combiner Ring,” Proc. of the 7th European Particle Accelerator Conference, June 26–30, 2000, Vienna, Austria and CLIC Note 471 (2001).
- [8] D. Alesini, R. Corsini, A. Gallo, F. Marcellini, D. Schulte, I. Syratchev, “Studies on the RF Deflectors for CTF3,” Proc. of the 7th European Particle Accelerator Conference, June 26–30, 2000, Vienna, Austria and CLIC Note 472 (2001).
- [9] H.H.Braun for the CTF Team, “Experimental results and technical research and development at CTF2,” Proc. 7th Eur. Part. Accel. Conf. (EPAC2000), Vienna, 2000.
- [10] M. Dehler, I. Wilson, W. Wuensch, “A Tapered Damped Accelerating Structure for CLIC,” CERN/PS 98-040 (LP), Proc. of the XIX Linac Conference, August 23–28, 1998, Chicago, USA.
- [11] R. Assmann: “Proposal for a CLIC Study of Final Focus Stabilization Technology and Time-Dependent Luminosity Performance.” Unpublished. Available at <http://www.cern.ch/clic-stability>

## BIBLIOGRAPHY FOR CHAPTER 5

- [12] R. Assmann et al, “Status of the CLIC Study on Magnet Stabilization and Time-dependent Luminosity Performance,” Proc. of EPAC2002 (Paris).